Chemistry–A European Journal
Research Article
doi.org/10.1002/chem.202404418
Chemistry Europe
European Chemical Societies Publishing
www.chemeurj.org

Synthesis, Photophysical, and Chemiexcitation Properties of Luminol-Fullerene Dyads: Toward Chemiexcitation Electron Transfer

Theodoros Mikroulis,[a] Gemma M. Rodríguez-Muñiz,[b] Demeter Tzeli,[c, d] Georgios Rotas,*[a, e] Miguel A. Miranda,*[b] and Georgios C. Vougioukalakis*[a]

Fullerene-based donor-acceptor (D-A) dyads have been extensively studied for their unique electronic properties, with applications in photoinduced energy conversion devices. In these systems, dynamic quenching of the excited donor's emission occurs, via energy or electron transfer to the fullerene acceptor. However, there are no reports on fullerene dyads bearing chemiluminescent donor analogues. In this context, the synthesis of two luminol-fullerene D-A dyads, bridged with alkyl chains of different lengths, is reported herein. The electronic communication between the two moieties was thoroughly evaluated, following either the photo- or chemi-excitation of the linked units. Steady state and time-resolved absorption studies, combined with emission techniques, were employed to monitor the deactivation fate of excited species. In general, a significant quenching of the excited luminol-derived emission signals was observed, revealing detectable intramolecular interactions between the two moieties. Unlike what is usually observed in other luminol-based D-A systems, quenching of the excited species generated upon photo- and chemi-excitation of the luminol-fullerene dyads is attributed to electron rather than energy transfer. This was found to be consistent with the estimated Gibbs energy of photoinduced electron transfer and with DFT theoretical calculations.

1. Introduction

Electronic communication between molecules, or moieties within a single molecule, is the cornerstone of energy transfer and conversion processes, occurring in both natural and artificial systems of energy harvesting and exploitation. Ranging from natural photosynthesis[1] to artificial organic photovoltaics,[2] photoinduced energy/electron transfer systems convert (sun)light energy to electricity, through the electronic communication between donor and acceptor (D-A) molecular entities. As a prerequisite, the proper selection of D and A, as well as the medium in which they communicate, is of paramount importance for the transfer outcome, given that the degree of communication affects both the mode and the yield of the transfer event. In this respect, fullerenes are considered among the best electron acceptors and have been used in the construction of organic photovoltaics for more than a decade. Their 3D spherical structure is responsible for their unique electronic properties, such as high electron affinity and transport, low reduction potential, and small reorganization energy in electron transfer processes.[3]

Chemiluminescence (CL) is the phenomenon where chemical energy is converted into light, generally through a series of redox reactions, following a chemical stimulus. Upon chemiexcitation, excited state species are produced, which deactivate via fluorescence or phosphorescence emission. This effect is applicable in a variety of fields, where fast response and high signal-to-noise ratio are needed, including analytical tools, bioimaging, immunoassays, and theranostics.[4] Luminol is probably the most notorious CL molecule, as it is stable, low-cost, and can trigger a bright CL, centered at 425 nm, as a result of the emission of the chemiexcited 3-aminophthalate.[5] In this respect, the need for lower energy CL-induced light has led to the construction of luminol based D-A systems (attached either covalently or noncovalently), where the luminol chemiexcited

[a] Dr. T. Mikroulis, Prof. Dr. G. Rotas, Prof. Dr. G. C. Vougioukalakis
Department of Chemistry, National and Kapodistrian University of Athens, Panepistimiopolis, 15771 Athens, Greece
E-mail: rotasgiorgos@uoi.gr
vougiouk@chem.uoa.gr

[b] Dr. G. M. Rodríguez-Muñiz, Prof. Dr. M. A. Miranda
Instituto de Tecnología Química UPV-CSIC, Universitat Politècnica de València, 46022 Valencia, Spain
E-mail: mmiranda@gim.upv.es

[c] Prof. Dr. D. Tzeli
Department of Chemistry, Laboratory of Physical Chemistry, National and Kapodistrian University of Athens, Panepistimiopolis, 15771 Athens, Greece

[d] Prof. Dr. D. Tzeli
Theoretical and Physical Chemistry Institute, National Hellenic Research Foundation, 11635 Athens, Greece

[e] Prof. Dr. G. Rotas
Department of Chemistry, Laboratory of Organic Chemistry, University of Ioannina, 45110 Ioannina, Greece

Supporting information for this article is available on the WWW under https://doi.org/10.1002/chem.202404418

species transfer their energy through Chemiluminescence Resonance Energy Transfer (CRET) to the acceptor moieties, which finally emit at longer wavelengths. Acceptors such as BODIPY,[6] fluorescein,[7] tetraphenylethene,[8] $Ru(bpy)_3^{2+}$,[9] or quantum dots[10] have been employed in luminol-based D-A conjugates, exhibiting energy transfer properties.

We herein report the synthesis, photophysical, and chemiluminescent properties of two luminol-fullerene D-A systems, where the two active moieties are covalently attached via flexible linear chain bridges of different lengths. By combining, for the first time, the strong CL efficiency of luminol with the unique energy/electron accepting properties of fullerene,[3g] the aim is to investigate whether a possible electronic communication between the two moieties can yield energy transfer and/or electron transfer, leading to charge separated states (CSSs) depending on the interchromophore chain length and interaction medium. To the best of our knowledge, electron transfer has never been reported as a deactivation pathway of chemiexcited luminol. The existence of such a pathway may lead to novel, stimuli-responsive materials, among others.

2. Results and Discussion

The synthesis of the fullerene-luminol dyads posed significant difficulties. The huge difference in the solubility of the two moieties (fullerene and fullerene derivatives are practically insoluble in polar solvents, while luminol is insoluble in nonpolar solvents) limited the options for the selection of the appropriate compounds to be coupled (fullerene and luminol derivatives), as well as the coupling conditions. For example, attempts to prepare dyads using the standard azomethine ylide cycloaddition[11a,b] reaction between C_{60} and a luminol amino acid or a luminol carboxaldehyde derivative, failed. We then opted for the use of a polar fullerene derivative as coupling partner. Again, no reaction was observed between a fullerene carboxylic acid and an amino-luminol derivative, either via acid chloride, or peptide coupling conditions. We managed to get the desired dyads **4a** and **4b** from the amide coupling reaction between amino-fullerene **3**[12] (in the form of an ammonium salt) and luminol-carboxylic acids **2a** and **2b**, respectively (Scheme 1). Acids **2** were prepared from the *N*-alkylation of luminol with the appropriate bromoalkyl carboxylic acids. The two derivatives **4a** and **4b** were thus successfully obtained from the coupling reaction, using EDC in DMF as solvent, albeit in very low yields, with unreacted starting materials mostly recovered. Compounds **4a** and **4b** were characterized using ^{1}H-NMR spectroscopy and MALDI-TOF spectrometry. The coupling products' ^{1}H-NMR spectra exhibit the peaks of both chromophores (characteristic: luminol aromatics and fulleropyrrolidine methylene's singlet at 4.5 ppm), while the newly formed amide NH emerging as broad triplets at around 8.1 ppm. They both exhibit very low solubility in every possible solvent. Additionally, the acetamide fullerene derivative **5** was prepared, as reference for the photophysical studies. Experimental details on the synthesis and characterization of the target compounds can be found in the SI (Supporting Information), sections S0 and S1.

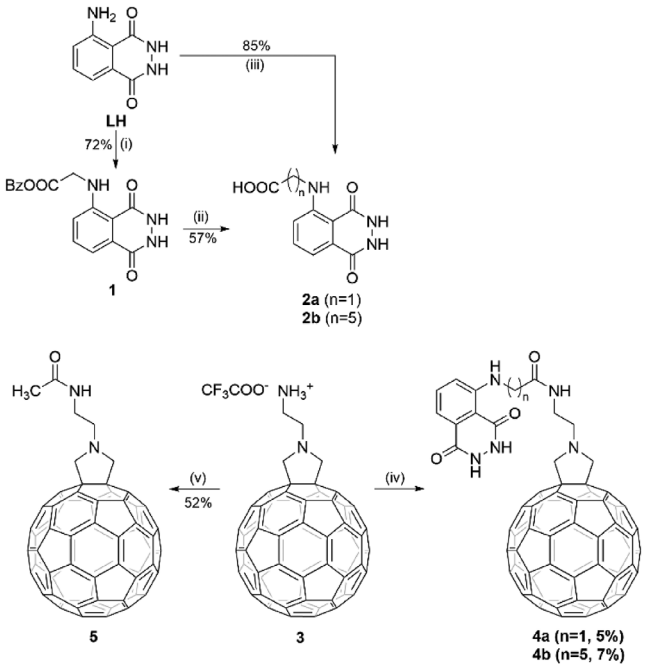

Scheme 1. Reagents and conditions: (i) benzyl bromoacetate, NMP, 110 °C, 1 hour, (ii) H_2, Pd/C, MeOH, r.t., 18 hours, (iii) 6-bromohexanoic acid, NMP, 110 °C, 72 hours, (iv), **2a** or **2b**, EDC, N-methylmorpholine, DMF, r.t. 48 hours, (v), AcOH, EDC, N-methylmorpholine, DMF, r.t. 48 hours.

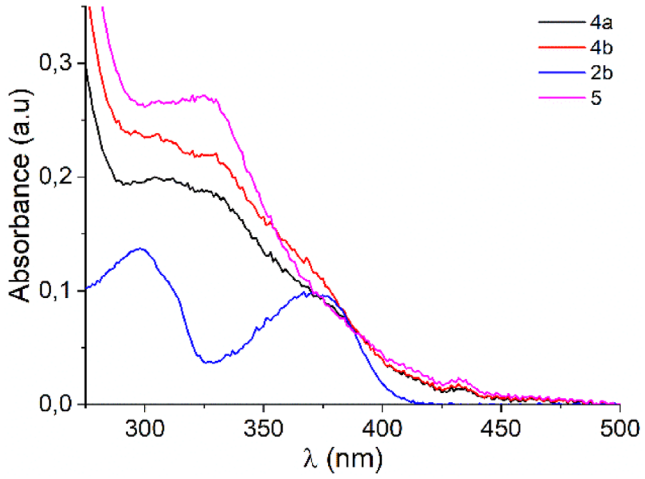

Figure 1. Absorption spectra of **4a**, **4b**, **2b**, and **5** in DMSO at 5 μM concentration.

To determine the response of the two dyads in CL-related processes, the electronic communication between the two moieties (luminol and fullerene) in both the ground and the excited states was examined first in DMSO, as this is the organic solvent of choice for CL experiments. In this respect, the absorption spectra of the two dyads **4a** and **4b** in DMSO were acquired, along with those of the reference compounds **2b** and **5**, which contain the separated chromophores (Figure 1). Not surprisingly, compounds **4a** and **4b** showed absorption peaks at ca. 310, 330, and 370 nm, reproducing the combined spectral characteristics of their constituent units **2b** (300 and 370 nm) and **5** (325 nm); however, the broad shape of the absorption spectra

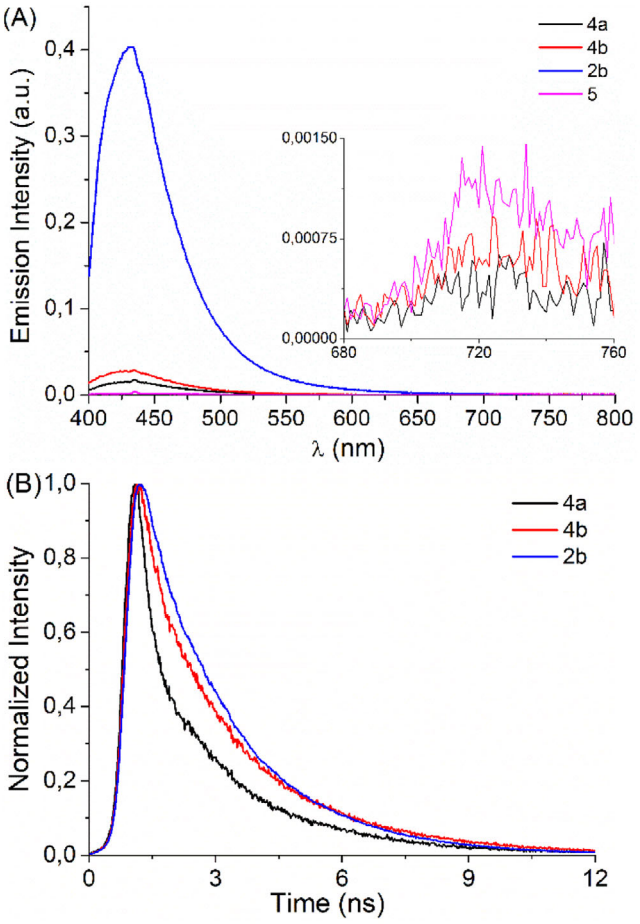

Figure 2. a) Steady state fluorescence emission spectra of **4a**, **4b**, **2b**, and **5**. Inset: expansion between 680–760 nm. b) Normalized emission decay traces at 435 nm of **4a**, **4b**, and **2b** in DMSO (λ_{ex} = 385 nm).

Table 1. Photophysical data obtained for luminol derivative **2b** and dyads **4a** and **4b**.

	τ_s [ns] [mono-exp fit] [R^2][a]	τ_{s1}/τ_{s2} [ns] [bi-exp fit] [R^2][a]	Relative Abundance [A1/A2]	k_{intra} [s^{-1}][b]
2b	2.08 (0.99993)			
4a	1.40 (0.97768)	0.39/2.30 (0.99853)	90/10	2.13×10^9
4b	1.99 (0.98662)	0.44/2.34 (0.99902)	69/31	1.85×10^9

[a] R^2 = Adjusted R-Square.
[b] The intramolecular quenching constant (k_{intra}) has been calculated as $k_{intra} = 1/\tau_1 - 1/\tau_2$.

of **4a** and **4b**, together with their failure to match the added spectra of **2b** and **5**, strongly suggested a considerable degree of aggregation.[13] In order to confirm that aggregation can be attributed to the covalently linked systems, rather than to their isolated components, absorption spectra were recorded upon addition of the parent fullerene to unsubstituted luminol, revealing the absence of the characteristic features associated with aggregation (see Figure S7 in the Supporting Information).

The steady- state emission properties were then evaluated (Figure 2a). Upon excitation of a DMSO solution, luminol **2b** showed a strong fluorescence emission band, centered at ca. 430 nm. Conversely, fullerene **5** showed a weak emission band, centered at ca. 720 nm. This is in good agreement with the known emission properties of luminols[11c] and fullerenes.[11d,e] Regarding the emission spectra of the dyads, upon excitation of **4a** at 385 nm, both the strong luminol emission at 420 nm, as well as the weak fullerene one at 720 nm were observed. Upon comparing the emission of **4a** and **4b** at 420 nm with that of **2b** (at the same concentration) using the same absorbance at the excitation wavelength, a dramatic quenching was observed for luminol emission in dyad **4a** and (to a somewhat lesser extent) in **4b**. This may be due to a static quenching associated with aggregation and/or to a dynamic quenching, which would reveal electronic communication between the two chromophores in the excited state. In the latter case, considering the fact that the two dyads differ only in their bridge length, this feature could contribute to the difference in the emission spectra. Additionally, upon excitation at 385 nm, fullerene emission at 720 nm was not enhanced in **4a** and **4b**, as compared with **5** (see Figure 2a, inset).

Photophysical measurements were also performed in toluene, which is in general considered a better solvent for fullerene derivatives. Under these conditions, although aggregation was still observed in the absorption spectra, the signals for the long-wavelength fullerene emission were less noisy, and emission quenching occurred to a lesser extent (see Supporting Information, Figures S8 and S9). This is consistent with the influence of relative solvent polarities on an electron transfer mechanism. Overall, the above observations point once again to a charge transfer pathway for fluorescence quenching and do not support energy transfer from excited luminol to fullerene moieties. Moreover, in these D-A systems, the overlap between the donor emission spectrum and the acceptor absorption spectrum (a requirement for efficient FRET) is very poor and makes the process unlikely.

To better understand the photophysical behavior of **4a** and **4b**, time-resolved experiments were then performed. The emission decay traces of dyads **4a** and **4b** are shown in Figure 2b, together with that of luminol **2b**. Although the decay of both dyads was faster than that of the reference compound **2b**, (see Supporting Information Figure S10), the differences were less remarkable than those observed in the steady-state experiments, where the contribution of static quenching appears to be much higher, likely due to aggregation. Nonetheless, the variations in the decay kinetics were consistent with a certain degree of dynamic quenching, which was more marked in the case of **4a**.

A deeper insight was obtained from the fluorescence lifetimes (τ_F) obtained upon fitting of the decay traces (Figure 3 and Table 1). In the case of **2b** a good mono-exponential fitting was observed, with a value τ_F of 2.08 ns (see Supporting Information, Figure S10). For **4a** and **4b**, it was necessary to introduce two lifetimes in order to achieve a satisfactory fitting. The numerical values were 0.39/2.30 ns for **4a** and 0.44/2.34 ns for **4b**. The longer component in both dyads is very similar to that of luminol derivative **2b**, remaining close to 2 ns. In contrast, the shorter

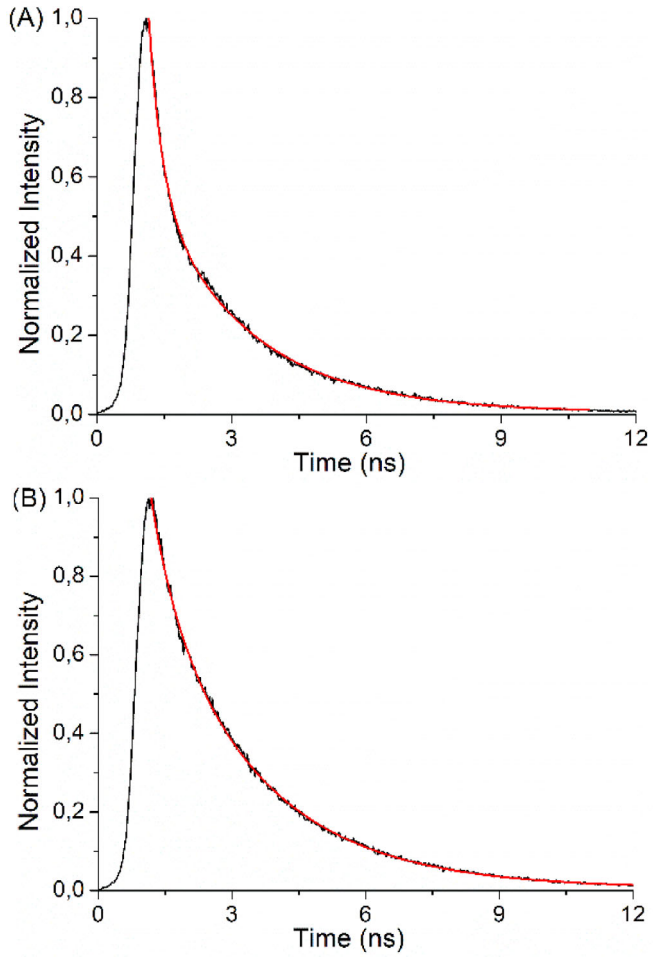

Figure 3. Black: Normalized emission decay traces at 435 nm a) **4a** b) **4b** in DMSO (λ_{ex} = 385 nm). Red: bi-exponential fitting using equation $y = A1*e^{-x/t1} + A2*e^{-x/t2}$.

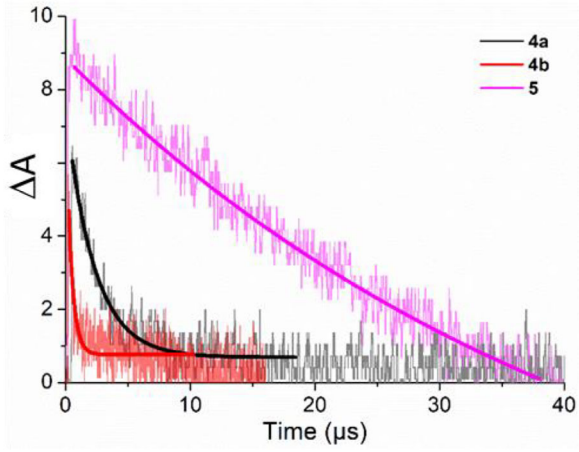

Figure 4. Flash photolysis smoothed spectral decay (at 690 nm in DMSO, under N_2) of **4a**, **4b**, **5** (λ_{ex} = 340 nm).

component shows a lower τ_F value (*ca.* 0.4) and its contribution is higher in **4a** than in **4b**. A reasonable explanation would be that the compound with the shorter bridge (**4a**) presents a higher number of active conformations, where the two interacting moieties are at close distance (shorter than 10 Å), which is a requirement for effective electron transfer (but much less for singlet energy transfer, where the Förster mechanism is less dependent on the interchromophoric distance).

The weak fluorescence efficiency of fullerenes is due to their efficient intersystem crossing, so C_{60} is known to show a triplet quantum yield close to unity.[11a,b] Furthermore, only a tiny fraction of singlet excited fullerene returns to the ground state via radiative and nonradiative processes. Hence, fullerene excited state is dominated by the deactivation of its triplet state. Accordingly, laser flash photolysis measurements were employed to shed light on the fate of fullerene's triplet excited state, by monitoring the triplet transient decay at 690 nm (Figure 4). The absorption maximum of this species in DMSO appeared around 700 nm (see Supporting Information, Figure S11), in close agreement with related literature precedents. [14] Fullerene derivative **5** showed a signal with a lifetime of 42 μs.[15] In the case of the dyads, the same signal decays much faster: **4a** decayed in 2.13 μs, while **4b** in just 0.35 μs. This fast decay of the triplet fullerene state points again the formation of a Charge Separated State (CSS, via Charge Transfer), stabilized in the polar solvent DMSO. The intramolecular triplet quenching constant (k_{intra}) can be calculated as $k_{intra} = 1/\tau$(4a or 4b) $-1/\tau$ (5), resulting in 4.45×10^5 and 2.83×10^6 s^{-1}, respectively. For comparison, the corresponding values in toluene, determined from the triplet decay kinetic traces (see Supporting Information, Figure S12), were 2.56×10^4 and 3.84×10^4 s^{-1}, respectively. Thus, the rate constants for triplet quenching decreased with decreasing solvent polarity, in agreement with an electron transfer mechanism, and were markedly lower than the abovementioned singlet counterparts. As a background reference, the transient spectra of the parent C_{60}, along with the decay kinetics in the presence of increasing concentrations of oxygen and of the unsubstituted luminol, are shown in Figures S13, S14, and S15 of the Supporting Information.

Although the intrinsic limitations of the employed systems (time resolution, spectral overlap, wavelength detection windows, etc.) did not allow us to achieve direct experimental detection of the possible mechanistic intermediates, further support for the proposed mechanism was obtained from estimations made on the Gibbs energy of photoinduced electron transfer from the singlet excited state of the parent luminol to the unsubstituted C_{60} fullerene in its ground state, using the known literature values for reduction potentials and excited state energies. Similar estimations were made on the photoinduced electron transfer from the ground sate of the parent luminol to the triplet excited state of the unsubstituted C_{60} fullerene.[16] The obtained results (see details in Supporting Information, Equations **2a**, **2b**, and Figure S16) showed that both processes are indeed thermodynamically allowed, thus reinforcing the feasibility of intramolecular electron transfer as the dynamic quenching mechanism in the investigated dyads.

We may then sum up our observations in a possible scenario for the main deactivation pathways, following excitation, as shown in Scheme 2. Due to the spectral overlap of the fullerene and luminol moieties in the Lum-Ful dyads, both luminol and fullerene can get excited, yielding ^{1}Lum*-Ful and Lum-^{1}Ful*, respectively. Both species may deactivate toward the ground

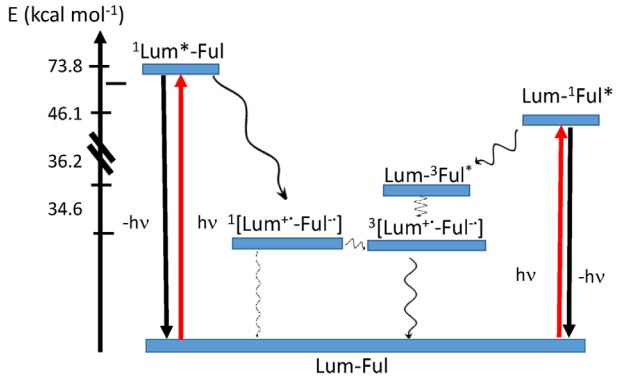

Scheme 2. Energy diagram for Luminol-Fullerene (Lum-Ful) dyads, following light excitation.

state, emitting light. Additionally, Lum-^{1}Ful* may yield Lum-^{3}Ful* through intersystem crossing. The polar solvent lowers the energy of the CSS, facilitating charge transfer from ^{1}Lum*-Ful or from Lum-^{3}Ful*, to give the CSSs with singlet or triplet multiplicity ^{1}(Lum$^{+\cdot}$-Ful$^{-\cdot}$) or ^{3}(Lum$^{+\cdot}$-Ful$^{-\cdot}$), respectively. Subsequent charge recombination may lead to Lum-Ful.

Having in hand the results from light excitation, we extended our study to the CL reactions of the dyads. In order to trigger CL, solutions of **2b**, **4a**, and **4b** were prepared in DMSO, with a concentration of 5 μM. Two milliliters of each solution was placed in a quartz cuvette, and the CL reaction was triggered by the addition of potassium *tert*-butoxide under vigorous stirring. The process was monitored using a fluorometer running in the time-based mode (with its own lamp switched off, and 430 nm as the monitoring wavelength). A control experiment demonstrated that the fullerene moiety is stable under the employed basic conditions (Supporting Information, Figure S17).

Chemiluminescence kinetics for **2b** and the luminol based dyads **4a** and **4b**, monitoring emission at 430 nm (Figure 5, top), showed a drastic CL signal weakening imposed by the fullerene. Upon integration, the total signal of the dyads as compared to **2b** is 23-fold weaker for **4a** and 28-fold for **4b**. At the present stage, the reason for this quenching is not fully understood. Luminol CL quenching in **4a** and **4b** is more complex than the fluorescence quenching studied above. At first, the CL emissive species is not luminol, but the excited aminophtalate ion, produced by luminol's oxidation reaction.[17] Thus, a different deactivation mechanism, compared to luminol, is possible. Additionally, the fluorescence quantum yield (Φ_F) of the emissive species is only one factor affecting the signal, since CL quantum yield (Φ_{CL}) is the product of reaction (Φ_R), chemiexcitation (Φ_{CE}), and fluorescence (Φ_F) quantum yields, each contributing to the observed signal intensity.[4c] Some more information is shown in Figure 5 (bottom), which depicts the rough CL emission spectra for **4a** and **4b**. These were not obtained by direct scanning, but instead from the combination of repeated CL experiments, averaging emission signals in particular wavelengths at specific time intervals, after CL triggering. In spite of the limitations and potential experimental errors associated with this experimental procedure, it seems obvious that the highest emission intensities fall in a region similar to that of luminol

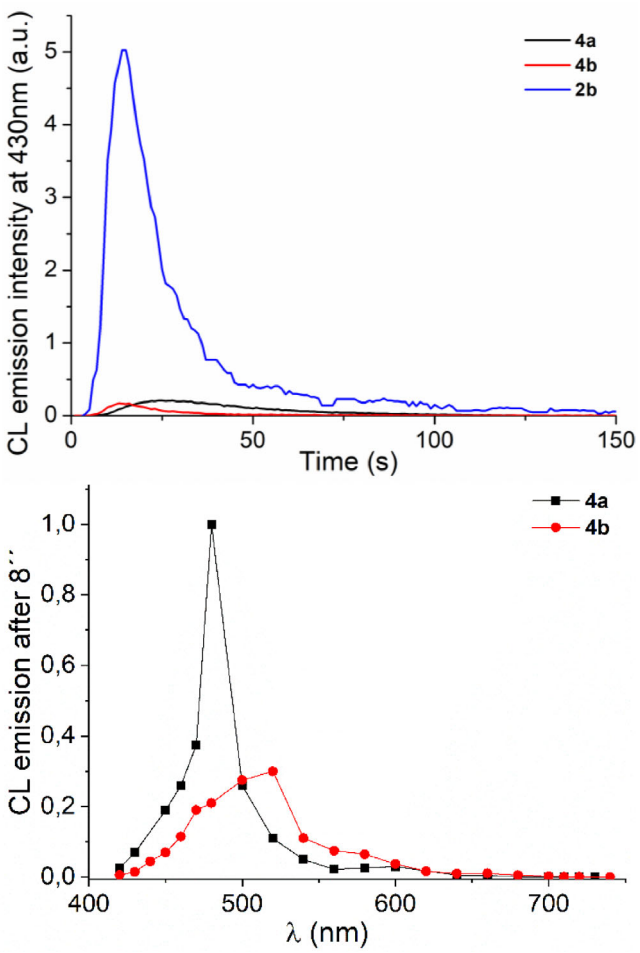

Figure 5. Top: CL kinetics of **4a**, **4b**, and **2b** (5 μM) monitoring emission at 430 nm. Bottom: Depiction of CL emission spectra of **4a** and **4b**, as constructed from CL emission decay signals.

CL (around 500 nm)[17,18] and far from the typical fluorescence of fullerene (ca. 700 nm). Finally, the relatively smaller spectral overlap of fullerene absorption with 3-aminophthalate emission as compared with luminol, can be one of the reasons for the lack of detectable energy transfer. In any case, energy transfer to fullerene does not seem to be a significant pathway for the observed luminol CL quenching. In this respect, and in line with the fluorescence experiments, electron transfer leading to a CSS is probably the most reasonable scenario.

In order to gain a deeper understanding of the obtained experimental results, a DFT conformational analysis was conducted for **2b**, **4a**, **4b**, and **5** at the M06-2X[19]/6–31G(d,p)[20] methodology in DMSO. The solvent was included as a dielectric constant via the polarizable continuum model,[21] which reproduces solvent effects well.[22] The absorption spectra of the lowest energy conformers were calculated via M06-2X,[19] and PBE0[23] functionals. The M06-2X functional was selected for the geometry optimization, because it predicts very well the π–π interactions.[19,24] The PBE0 functional has been tested for its ability to predict excited state properties, including vertical excitation energies and excited state geometries.[25] Its performance has been compared to other functionals for predicting

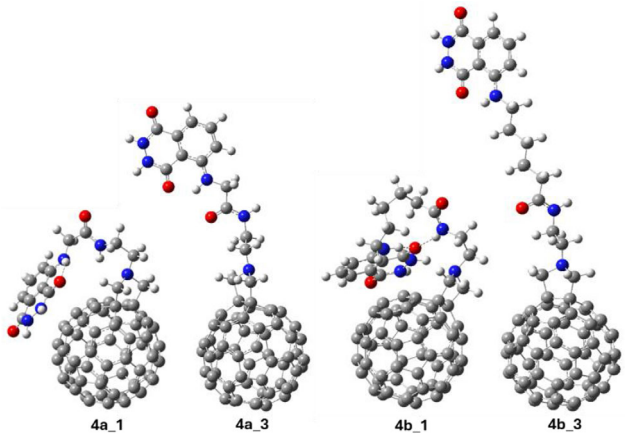

Figure 6. Lowest energy (_1) and extended chain (_3) calculated conformers of **4a** and **4b** at the M06-2X/6–31G(d,p) in DMSO solvent.

vertical excitation energies of singlet excited states, leading to the conclusion that this is among the most effective functionals regarding the average deviation.[25] The absorption spectra of the molecules were calculated including up to 60 lowest-in-energy excited singlet-spin electronic and up to 50 lowest-in-energy excited triplet-spin electronic states. All calculations were carried out via Gaussian16.[26] The calculated geometries are given in Table S1 of the Supporting Information.

The most relevant conformers of **2b**, **4a, 4b**, and **5** are shown in Figure 6 and Figure S18 of the Supporting Information. In the lowest energy conformers of **4a** and **4b**, that is, **4a_1** and **4b_1** (Figure 6), respectively, the spacers bend, in order for $\pi-\pi$ favorable interactions to take place between the luminol and C_{60}, moieties; the distance of these $\pi-\pi$ interactions is about 3.2 Å. Moreover, NH…O and NH…N interactions are also into play, stabilizing some unfolded conformers, such as **4a_3** (5.6 kcal/mol above **4a_1**) or **4b_3** (10.5 kcal/mol higher in energy than **4b_1**) (Figure 6; all calculated conformers are shown in the Supporting Information, Figure S18). This suggests that in solution **4a** and **4b** prefer to adopt the folded conformation in which $\pi-\pi$ interactions are present, thus making it possible for intramolecular electron transfer to occur.

The $\pi-\pi$ interactions are also observed at the H-1 and H molecular orbitals of the **4a_1** and **4b_1** conformers (Figure 7; all calculated conformers are shown in the Supporting Information, Figure S19). The five H-4, H-3, H-2, H-1, and H molecular orbitals of **4a**, **4b** and **5** are almost energetically degenerate. The H-4, H-3, and H-2 correspond to molecular orbitals with electronic density located only on C_{60}. The H-1 orbital of **4a_3** and **4b_3** where $\pi-\pi$ interactions are not formed, present electron density on luminol only. On the contrary, for the **4a_1** and **4b_1** conformers, their H-1 orbital present electron density in both luminol and C_{60} due to $\pi-\pi$ interactions. The H orbital of **4a_1** presents electron density only on C_{60}, while the H orbital of **4b_1** presents electron density on both luminol and C_{60}. It should be mentioned that the energy difference of H-4 and H is about 0.25 eV for **4a_1** and **4b_1**. Thus, many close lying excitations are observed. The electron density of the lowest in energy LUMO orbitals, L, L + 1 are located only on C_{60}.

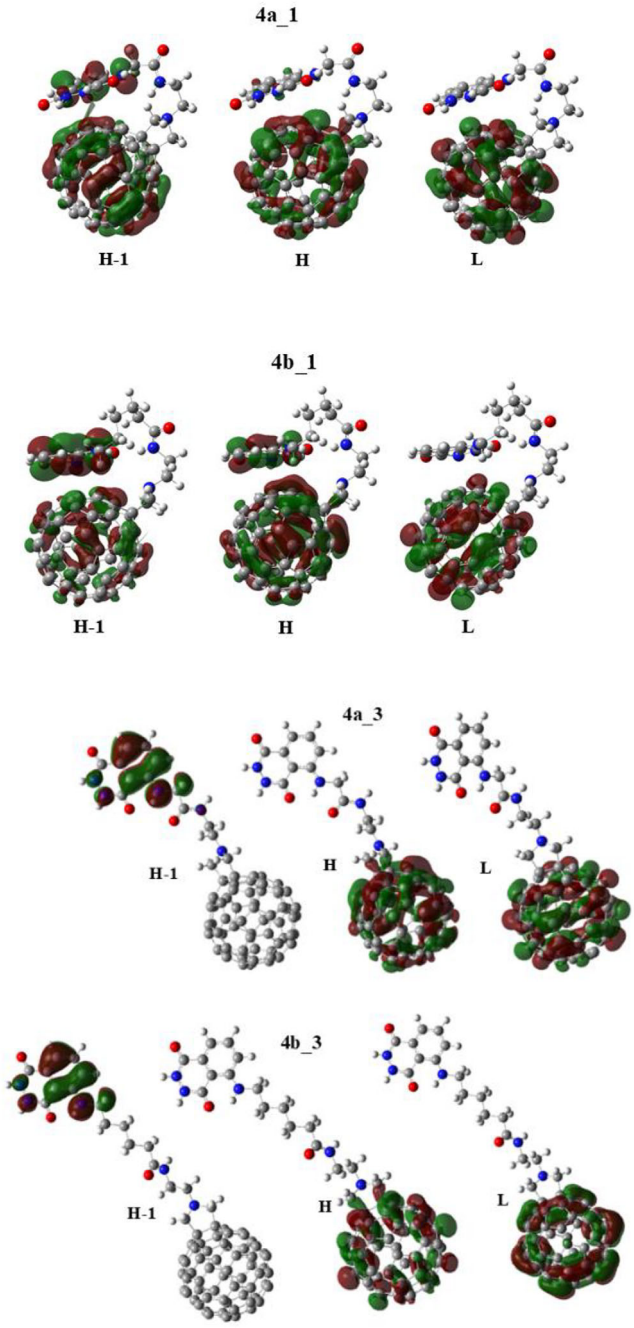

Figure 7. Frontier Molecular orbitals of two calculated conformers of **4a** and **4b**.

As a general observation, the shape of the UV-vis absorption spectra using the two functionals was the same and in reasonable agreement with our experimental spectra (Supporting Information, Figures S20 and S21). M06-2X calculates absorption peaks that are blue shifted with respect to the corresponding PBE0 calculated peaks. These blue shifts of M06-2X compared to PBE0 have been observed in other molecules, while generally PBE0 predicts the same absorption peaks as the B3LYP functional.[25,27] Experimentally, **4a**, **4b**, and **5** present an absorption band at about 330 nm. Computationally, M06-2X functional calculates an absorption band at 310 nm, while the PBE0

functional, when 50 singlet excited states have been calculated, presents an absorption band at about 340 nm. Thus, the best agreement between the calculated absorption spectra with the experimental ones is observed using the PBE0 functional.

Finally, for **4a**, **4b**, and **5** minima, their PBE0 vertical $S_0 \rightarrow S_1$ and $S_0 \rightarrow S_2$ excitations are at about 2.03 eV (= 610 nm) and 2.14 eV (= 580 nm), respectively, while their T_1 and T_2 are lying at about 1.51 eV (820 nm) and 1.65 eV (750 nm) above the S_0 state, respectively, supporting the energy diagram of Scheme 2. Geometry optimization of their T_1 state shows that the adiabatic energy difference between the S_0 and T_1 states is 1.20 eV (= 1333 nm). Note that, the geometries of the S_0 and T_1 states are very similar, but they are not the same.

3. Conclusion

Two fullerene-luminol dyads (**4a** and **4b**) having flexible bridges of different lengths, have been synthesized in order to evaluate their photophysical and chemiluminescent properties. Considerable solubility issues were confronted, imposing low synthetic yields and limitations to full spectroscopic studies. Nevertheless, steady- state absorption and emission studies of the dyads, following their photoexcitation in DMSO solutions, reveal a remarkable luminol fluorescence quenching. Although a major contribution to this quenching seems to be static (attributed to aggregation), the parallel shortening of the emission lifetimes, observed in time-resolved studies, confirms that the quenching process is partially of dynamic nature, becoming enhanced in the case of the shorter bridge derivative **4a**, as compared with the longer chain analogue **4b**. The obtained results are in agreement with a thermodynamically allowed intramolecular charge transfer, which requires a close proximity between the two intervening moieties, as compared with resonance singlet energy transfer. The absence of fullerene emission enhancement, along with the fast deactivation of fullerene triplet excited state, reinforces the proposed electron transfer deactivation mechanism. In addition, CL monitoring of **4a** and **4b**, shows a sharp decrease of the CL signal in the luminol region, as compared to parent luminol. The total absence of fullerene emission suggests again electron transfer as the main intramolecular deactivation pathway. The design and synthesis of related molecules with improved solubility in polar solvents is expected to diminish aggregation, thus shedding more light on the materials' photophysics. As a result, possible applications in energy conversion scaffolds, by diverting chemiexcitation energy in useful pathways, other than CL, may arise.

Supporting Information

Details of experimental and synthetic procedures, identification spectra, and supplementary figures are provided in Supporting Information.

Acknowledgments

This project was financially supported by the European Union's Horizon 2020 framework program for research and innovation under grant agreement no. 712921.

Conflict of Interest

The authors declare no conflict of interest.

Data Availability Statement

The data that support the findings of this study are available in the supplementary material of this article.

Keywords: chemiluminescence · donor-acceptor · electron transfer · fullerene · luminol

[1] T. Mirkovic, E. E. Ostroumov, J. M. Anna, R. van Grondelle, Govindjee, G. D. Scholes, *Chem. Rev.* **2017**, *117*, 249.
[2] a) C. J. Brabec, N. S. Sariciftci, J. C. Hummelen, *Adv. Funct. Mater.* **2001**, *11*, 15; b) S. H. Park, A. Roy, S. Beaupré, S. Cho, N. Coates, J. S. Moon, D. Moses, M. Leclerc, K. Lee, A. J. Heeger, *Nat. Photonics* **2009**, *3*, 297; c) N. Gasparini, A. Salleo, I. McCulloch, D. Baran, *Nat. Rev Mater.* **2019**, *4*, 229.
[3] a) C.-Z. Li, H.-L. Yip, A. K. Y. Jen, *J. Mater. Chem.* **2012**, *22*, 4161; b) S. Collavini, J. L. Delgado, *Sustainable Energy Fuels* **2018**, *2*, 2480; c) R. Ganesamoorthy, G. Sathiyan, P. Sakthivel, *Sol. Energy Mater. Sol. Cells* **2017**, *161*, 102; d) Z. Zhou, S. Xu, J. Song, Y. Jin, Q. Yue, Y. Qian, F. Liu, F. Zhang, X. Zhu, *Nat. Energy* **2018**, *3*, 952; e) M. Adnan, Z. Irshad, R. Hussain, W. Lee, M. Kim, J. Lim, *Sol. Energy* **2023**, *257*, 324; f) F. Zhang, K. Zhu, *Adv. Energy Mater.* **2019**, *10*, 1902579; g) D. M. Guldi, *Chem. Commun.* **2000**, 321.
[4] a) M. Yang, J. Huang, J. Fan, J. Du, K. Pu, X. Peng, *Chem. Soc. Rev.* **2020**, *49*, 6800; b) C. Dodeigne, L. Thunus, R. Lejeune, *Talanta* **2000**, *51*, 415; c) F. Barni, S. W. Lewis, A. Berti, G. M. Miskelly, G. Lago, *Talanta* **2007**, *72*, 896; d) D. Mao, W. Wu, S. Ji, C. Chen, F. Hu, D. Kong, D. Ding, B. Liu, *Chem* **2017**, *3*, 991; e) A. Pantelia, I. Daskalaki, M. Consuelo Cuquerella, G. Rotas, M. A. Miranda, G. C. Vougioukalakis, *Molecules* **2019**, *24*, 3957; f) T. Mikroulis, M. Consuelo Cuquerella, A. Giussani, A. Pantelia, G. M. Rodriguez-Muñiz, G. Rotas, D. Roca-Sanjuan, M. A. Miranda, G. C. Vougioukalakis, *J. Org. Chem.* **2021**, *86*, 11388.
[5] a) Y. Su, H. Song, Y. Lv, *Microchem. J.* **2019**, *146*, 83; b) P. Khan, D. Idrees, M. A. Moxley, J. A. Corbett, F. Ahmad, G. von Figura, W. S. Sly, A. Waheed, M. I. Hassan, *Appl. Biochem. Biotechnol.* **2014**, *173*, 333; c) M. Mayer, S. Takegami, M. Neumeier, S. Rink, A. Jacobi von Wangelin, S. Schulte, M. Vollmer, A. G. Griesbeck, A. Duerkop, A. J. Baeumner, *Angew. Chem. Int. Ed. Engl.* **2018**, *57*, 408; d) G. M. Rodriguez-Muniz, T. Mikroulis, A. Pantelia, G. Rotas, M. Consuelo Cuquerella, G. C. Vougioukalakis, M. A. Miranda, *Molecules* **2022**, *27*, 1245.
[6] a) H. Ning, Y. Yang, C. Lv, D. Zhou, S. Long, W. Sun, J. Du, J. Fan, X. Peng, *Nano Res.* **2023**, *16*, 12294; b) A. Degirmenci, O. Sonkaya, C. Soylukan, T. Karaduman, F. Algi, *ACS Appl. Bio. Mater.* **2021**, *4*, 5090.
[7] A. B. Solea, M. D. Ward, *Dalton Trans*. **2023** *52*, 4456.
[8] J. Lou, X. Tang, H. Zhang, W. Guan, C. Lu, *Angew. Chem. Int. Ed. Engl.* **2021**, *60*, 13029.
[9] J.-L. Liu, M. Zhao, Y. Zhuo, Y.-Q. Chai, R. Yuan, *Chem. - Eur. J.* **2017**, *23*, 1853.
[10] X. Huang, L. Li, H. Qian, C. Dong, J. Ren, *Angew. Chem. Int. Ed. Engl.* **2006**, *45*, 5140.
[11] a) F. Langa de la Puente, J.-F. Nierengarten, *Fullerenes: Principles and Applications*. The Royal Society of Chemistry: **2011**; b) F. Prat, R. Stackow, R. Bernstein, W. Qian, Y. Rubin, C. S. Foote, *J. Phys. Chem. A.* **1999**, *103*,

7230; c) R. Perez-Ruiz, R. Fichtler, Y. Diaz Miara, M. Nicoul, D. Schaniel, H. Neumann, M. Beller, D. Blunk, A. G. Griesbeck, A. Jacobi von Wangelin, *J. Fluoresc.* **2010**, *20*, 657; d) J. Catalan, J. Elguero, *J. Am. Chem. Soc.* **1993**, *115*, 9249; e) Y. Zhao, Y. Fang, Y. Jiang, *Spectrochim. Acta A* **2006**, *64*, 564.
[12] K. Kordatos, T. Da Ros, S. Bosi, E. Vazquez, M. Bergamin, C. Cusan, F. Pellarini, V. Tomberli, B. Baiti, D. Pantarotto, V. Georgakilas, G. Spalluto, M. Prato, *J. Org. Chem.* **2001**, *66*, 4915.
[13] a) N. O. Mchedlov-Petrossyan, M. O. Marfunin, N. N. Kriklya, *Liquids* **2024**, *4*, 32; b) G. Angelini, P. De Maria, A. Fontana, M. Pierini, M. Maggini, F. Gasparrini, G. Zappia, *Langmuir* **2001**, *17*, 6404.
[14] T. Nojiri, A. Watanabe, O. Ito, *J. Phys. Chem. A* **1998**, *102*, 5215.
[15] J. W. Arbogast, A. P. Darmanyan, C. S. Foote, F. N. Diederich, R. L. Whetten, Y. Rubin, M. M. Alvarez, S. J. Anz, *J. Phys. Chem.* **1991**, *95*, 11.
[16] a) Y. Zeng, L. Biczok, H. Linschitz, *J. Phys. Chem.* **1992**, *96*, 5237; b) G. Merenyi, J. Lind, X. Shen, T. E. Eriksen, *J. Phys. Chem.* **1990**, *94*, 748; c) L. Pospíšil, M. Hromadová, M. Gál, J. Bulíčková, R. Sokolová, S. Filippone, J. Yang, Z. Guan, A. Rassat, Y. Zhang, *Carbon* **2010**, *48*, 153.
[17] J. D. Gorsuch, D. M. Hercules, *Photochem. Photobiol.* **1972**, *15*, 567.
[18] J. Lee, H. H. Seliger, *Photochem. Photobiol.* **1970**, *11*, 247.
[19] Y. Zhao, D. G. Truhlar, *Theor. Chem. Acc.* **2008**, *120*, 215.
[20] L. A. Curtiss, M. P. McGrath, J. P. Blaudeau, N. E. Davis, R. C. Binning, L. Radom, *J. Chem. Phys.* **1995**, *103*, 6104.
[21] S. Miertuš, E. Scrocco, J. Tomasi, *Chem. Phys.* **1981**, *55*, 117.
[22] J. Tomasi, B. Mennucci, R. Cammi, *Chem. Rev.* **2005**, *105*, 2999.
[23] C. Adamo, V. Barone, *J. Chem. Phys.* **1999**, *110*, 6158.
[24] D. Tzeli, I. D. Petsalakis, G. Theodorakopoulos, *Phys. Chem. Chem. Phys.* **2011**, *13*, 11965.
[25] D. Jacquemin, A. Planchat, C. Adamo, B. Mennucci, *J. Chem. Theory Comput.* **2012**, *8*, 2359.
[26] M. J. Frisch, G. W. Trucks, H. B. Schlegel, G. E. Scuseria, M. A. Robb, J. R. Cheeseman, G. Scalmani, V. Barone, B. Mennucci, G. A. Petersson, et al. *Gaussian 16*, Revision C.01; Gaussian, Inc.: Wallingford, CT, USA, **2016**.
[27] C. Kolokytha, A. Sinani, T. Manouras, E. Angelakos, P. Argitis, N. N. Lathiotakis, C. Riziotis, D. Tzeli, *J. Phys. Chem. A* **2025**, *129*, 1219.

Manuscript received: November 29, 2024
Revised manuscript received: May 30, 2025
Version of record online: June 27, 2025